

Universiteit
Leiden
The Netherlands

# Aged human osteochondral explants as biomimetic osteoarthritis model: towards a druggable target in osteoarthritis

Houtman, E.

**Citation**
Houtman, E. (2022, October 12). *Aged human osteochondral explants as biomimetic osteoarthritis model: towards a druggable target in osteoarthritis*. Retrieved from https://hdl.handle.net/1887/3480151

| | |
|---|---|
| Version: | Publisher's Version |
| License: | Licence agreement concerning inclusion of doctoral thesis in the Institutional Repository of the University of Leiden |
| Downloaded from: | https://hdl.handle.net/1887/3480151 |

**Note:** To cite this publication please use the final published version (if applicable).

# Chapter 5

## Inhibiting thyroid activation in aged human explants prevents mechanical induced detrimental signalling by mitigating metabolic processes

Evelyn Houtman[1], Margo Tuerlings[1], H. Eka D. Suchiman[1], Nico Lakenberg[1], Frederique M.F. Cornelis[2], Hailiang Mei[3], Demiën Broekhuis[4], Rob G.H.H. Nelissen[4], Rodrigo Coutinho de Almeida[1], Yolande F.M. Ramos[1], Rik J. Lories[2, 5], Luis J. Cruz [6], Ingrid Meulenbelt[1]

*[1] Molecular Epidemiology, Department of Biomedical Data Sciences, Leiden University Medical Center, Leiden, The Netherland, [2] Department of Development and Regeneration, Skeletal Biology and Engineering Research Centre, Laboratory of Tissue Homeostasis and Disease, KU Leuven, Leuven, Belgium, [3] Sequencing Analysis Support Core, Leiden University Medical Centre, Leiden, The Netherlands, [4] Department of Orthopaedics, Leiden University Medical Center, Leiden, The Netherlands, [5] Division of Rheumatology, University Hospitals Leuven, Leuven, Belgium, [6] Translational Nanobiomaterials and Imaging (TNI) Group, Department of Radiology, Leiden University Medical Centrum, Leiden, the Netherlands*

**Published in**: Rheumatology (Oxford). 2022 Apr 5;keac202.
doi: 10.1093/rheumatology/keac202.

# Abstract

**Objectives**
To investigate whether the deiodinase inhibitor iopanoic acid (IOP) has chondroprotective properties, a mechanical stress induced model of human aged explants was used to test both repeated dosing and slow-release of IOP.

**Methods**
Human osteochondral explants subjected to injurious mechanical stress (65%MS) were treated with IOP or IOP encapsulated in poly lactic-co-glycolic acid (PLGA)-polyethylene glycol (PEG) nanoparticles (NP) (PLGA-PEG NPs (NP(IOP)). Changes to cartilage integrity and signalling were determined by Mankin scoring of histology, sulphated glycosaminoglycan (sGAG) release and expression levels of catabolic, anabolic and hypertrophic markers. Subsequently, on a subgroup of samples, RNA-sequencing was performed on 65%MS (n=14) and 65%MS+IOP (n=7) treated cartilage to identify IOP's mode of action.

**Results**
Damage from injurious mechanical stress was confirmed by increased cartilage surface damage in the Mankin score, increased sGAG release, and consistent upregulation of catabolic markers and downregulation of anabolic markers. IOP and, though less effective, PLGA NP(IOP) treatment, reduced *MMP13* and increased *COL2A1* expression. In line with this, IOP and PLGA NP(IOP) reduced cartilage surface damage induced by 65%MS, while only IOP reduced sGAG release from explants subjected to 65%MS. Lastly, differential expression analysis identified 12 genes in IOP's mode of action to be mainly invovled in reducing metabolic processes (*INSIG1*, *DHCR7*, *FADS1* and *ACAT2*), and proliferation and differentiation (*CTGF*, *BMP5* and *FOXM1*).

**Conclusion**
Treatment with the deiodinase inhibitor IOP reduced detrimental changes of injurious mechanical stress. In addition, we identified that its mode of action was likely on metabolic processes, cell proliferation and differentiation.



**Keywords**
Osteoarthritis, DIO2, chondrocytes, cartilage, thyroid signalling, iopanoic acid, mechanical stress

## Introduction

Osteoarthritis (OA) is a prevalent and debilitating age-related disease. It is a progressive disease characterized by cartilage degeneration and osteophyte formation [1]. Given the ageing society with increasing obesity rates, OA is projected to be the most frequent disease in the Dutch population in 2040, affecting 2.3 million people. Due to the fact that there is no effective treatment, except for joint replacement surgery, OA has a considerable social and economic burden on the ageing population.

Chondrocytes reside in healthy articular cartilage in a maturation-arrested state without detectable proliferation and with low metabolic activity [2]. Yet, with an inherently low tissue repair capacity of chondrocytes, the integrity of cartilage tissue is irreversibly affected upon environmental challenges such as injurious mechanical stress [3]. By applying molecular profiling of human OA articular cartilage, it has been consistently shown that activated articular chondrocytes with OA pathophysiology lose their healthy maturation-arrested state and recapitulate an activated growth plate morphology with associated debilitating gene expression [4]. To delineate underlying OA disease aetiology, large-scale genetic studies have been performed and provided further evidence that indeed genes orchestrating the endochondral ossification processes of growth plate chondrocytes could be, among others, a common underlying OA pathway [5]. Basing clinical development on functional data of OA risk genes could have measurable impact on development of effective disease modifying OA drugs given that the presence of genetically supported targets doubles the success rate of a drug in clinical development [6].



An example of such an OA risk gene is *DIO2*, encoding the deiodinase iodothyroinine type-2 (D2) [7]. D2 is an enzyme that converts intracellular thyroxine (T4) into triiodothyronine (T3) in specific tissues such as growth plate cartilage. Here, T3 initiates terminal maturation of hypertrophic chondrocytes leading to breakdown and mineralization of cartilage to allow transition to bone [8]. Functional genomic studies have demonstrated that the *DIO2* risk allele rs225014-C has an increased expression relative to the reference allele rs225014-T [9]. Moreover, in human preserved and lesioned OA articular cartilage, upregulated *DIO2* expression has been shown to be a common and consistent phenomenon, particularly relative to healthy cartilage [10]. *In vitro* 3D chondrogenesis with human bone marrow mesenchymal stem cells (hBMSC) indicated that overexpression of *DIO2* had a detrimental effect on matrix deposition while iopanoic acid (IOP), a potent inhibitor of deiodinases like D2, had beneficial effects on matrix deposition [11,12]. In line with this, *Dio2* knockout mice were protected from running induced joint damage [11]. Transgenic rats with cartilage-specific overexpression of human DIO2 (hD2Tg), did not show any articular cartilage defects [13]. However, upon increasing the biomechanical burden by applying an injury-induced OA model, hD2Tg rats showed significantly higher levels of cartilage damage compared with their wild-type littermates. Taken together, it was hypothesized that *DIO2* might confer risk to OA by affecting the propensity of maturation-arrested articular chondrocytes to recuperate growth plate morphology upon environmental challenges such as injurious mechanical stress. Additionally, IOP, a previously approved pharmaceutical agent, was delineated as mitigating this process [14].

The current study aimed to confirm chondroprotective effects of the D2 inhibitor IOP in a previously established *ex vivo* aged human osteochondral explant model in which injurious

mechanical stress is applied to inflict OA-like damage [15]. To improve treatment efficacy of the small IOP molecule, we investigated efficiency of IOP encapsulated in poly lactic-co-glycolic acid (PLGA)-polyethylene glycol (PEG) nanoparticles (NP) to establish slow prolonged release. Finally, RNA-sequencing was performed to explore the mode of IOP treatment action by addressing transcriptome-wide gene expression changes.

## Material and Methods

### *Study design and culture condition*

Osteochondral explants were obtained from knee joints included in the Research in Articular Osteoarthritis Cartilage (RAAK) study [16]. The RAAK study has been approved by the medical ethical committee of the Leiden University Medical Center (P08.239/P19.013) and informed consent was obtained from subjects. Osteochondral explants were punched from human OA knee joints and maintained in standard chondrogenic medium as described in Supplementary Materials and Methods, available at *Rheumatology* online. Medium was refreshed every 3–4 days. During mechanical stress, explants resided in phosphate buffered saline (PBS). In total 83 osteochondral explants were obtained from 16 donors for this study and divided over the following treatment groups: control (n = 30 explants; N = 16 donors), injurious mechanical stress (65%MS; n = 25 explants; N = 16 donors), injurious mechanical stress treated with IOP (65%MS+IOP; n = 11 explants; N = 6 donors) and injurious mechanical stress treated with NP-IOP (65%MS+NP-IOP; n = 17 explants; N = 10 donors). Donor characteristics are summarized in **Supplementary Table S1**, available at *Rheumatology* online.

### *Ethics*

Our study complies with the Declaration of Helsinki. Furthermore, the RAAK study has been approved by the medical ethical committee of the Leiden University Medical Center (P08.239/P19.013) and written informed consent was obtained from subjects.

### *Injurious mechanical stress model*

Six days after extraction, dynamic unconfined compression was applied at a strain of 65% of explant height at a frequency of 1 Hz using the Mach-1 mechanical testing system (Biomomentum Inc., Laval, QC, Canada) on four subsequent days as described previously (**Supplementary Figure S1**, available at *Rheumatology* online) [15].

### *IOP Treatment*

Explants were treated with IOP (100μM; Sigma) or 24ul of IOP encapsulated in PLGA-PEG nanoparticles (70μg IOP/mg NP; 5 mg NP/mL PBS) from day 3 onwards (**Supplementary Figure S1**). On day 13, cartilage and bone were separated using a scalpel, snap-frozen in liquid nitrogen and stored at -80 °C for RNA isolation. For histology, a part was fixed in 4% formaldehyde. Medium was collected on day 13 and stored at -80 °C. Details on sGAG

measurement, histology and PLGA NP characterization can be found in **Supplementary Materials and Methods**.

### *RNA isolation, Reverse Transcription and quantitative Real-Time PCR*

Cartilage RNA was extracted by pulverizing the tissue using a Mixer mill 200 (Retch, Germany) and homogenizing in TRIzol reagent (Invitrogen, San Diego, CA). RNA was extracted with chloroform, precipitated with ethanol, and purified using the RNeasy Mini Kit (Qiagen, GmbH, Hilden, Germany). Genomic DNA was removed by DNase (Qiagen, GmbH, Hilden, Germany) digestion and quantity of the RNA was assessed using a Nanodrop spectrophotometer (Thermo Fischer Scientific Inc., Wilmington, USA). Synthesis of cDNA was performed using 200 ng of total mRNA with the First Strand cDNA Synthesis Kit (Roche Applied Science, Almere, The Netherlands) according to the manufacturer's protocol. Subsequently, pre-amplification was performed and gene expression was determined with the Roche Lightcycler 480 II (Roche Applied Science) using Fast Start Sybr Green Master mix (Roche Applied Science). To measure changes in chondrocyte signalling upon perturbations, we measured gene expression levels by RT-qPCR. Primer sequences used are listed in **Supplementary Table S2**. Fold changes (FC) were determined using the $2^{-\Delta\Delta CT}$ method, in which cyclic threshold (CT) levels were adjusted for the housekeeping gene *SDHA* (-ΔCT) and subsequently for control samples (-ΔΔCT). A FC>1 represents an upregulation, while FC<1 depicts a downregulation.



### *RNA-sequencing*

Paired-end 2x150 base pair RNA sequencing (Illumina TruSeq mRNA Library Prep Kit, Illumina HiSeq X ten) was performed. Strand specific RNA-sequencing libraries were generated which yielded on average 14 million reads per sample. Data from the Illumina platform was analysed with an in-house pipeline as previously described [4]. See **Supplementary Materials** for detailed description of alignment, mapping, normalization and quality control. In total, 14.668 protein-coding genes were included in further analyses.

### *Differential expression analysis and protein-protein interactions*

Differential expression analysis was performed for 65%MS+IOP cartilage compared with 65%MS cartilage obtained from osteochondral explants using DESeq2 R package version 1.24 [17] on 14.668 protein-coding genes. A general linear model assuming a negative binominal distribution was applied and followed by a Wald-test between 65%MS+IOP and 65%MS samples with correction for principal component 1. In all analyses, 65%MS samples were set as reference. To correct for multiple testing the Benjamini-Hochberg method was used, as indicated by the false discovery rate (FDR) in which a significant cut-off value of 0.05 was used. For protein-protein interactions, analysis was performed using the online tool STRING version 11.0 [18].

### *RNA-sequencing validation by Real-time quantitative PCR (RT-qPCR)*

For validation and replication a total of 8 paired samples were selected. 200 ng of RNA was processed into cDNA using the First Strand cDNA Synthesis Kit (Roche Applied Science, Almere, The Netherlands). Real-Time qPCR was performed and normalized as described above to determine gene expression of *INSIG1*, *DHCR7*, *FADS1, CTGF*, *BMP*5 and *FOXM1*.

### *Statistical analysis*

RNA-sequencing data analysis was performed in R as described in **Supplementary Materials and Methods**. All other statistical analysis was performed using IBM SPSS statistics 25. *P*-values were determined by applying linear generalized estimating equation (GEE) to effectively adjust for dependencies among donors of the explants by adding a random effect for sample donor as we did not have perfect pairs for each analysis [19]. The following GEE was fitted in which gene expression was the dependent variable and treatment the covariate: *gene expression ~ treatment + (1|donor)*. To determine differences in sGAG concentrations on day 13, another linear GEE model was fitted with sGAG concentration as dependent variable and treatment as covariate: *sGAG concentration ~ treatment + (1|donor)*. Differences in Mankin score between groups was determined by applying the following linear GEE model with Mankin score as dependent variable and treatment as covariate: *Mankin score ~ treatment + (1|donor)*. Results are described by showing their fold change (FC) or average ± standard error (s.e.).

## Results

### *IOP reduces detrimental chondrocyte signalling induced by 65%MS*

First we confirmed that injurious mechanical stress (65%MS) induced detrimental changes to cartilage integrity of control and 65%MS aged human osteochondral explants [15]. Changes in chondrocyte signalling in response to 65%MS were determined by measuring gene expression levels of catabolic (*MMP13*, *ADAMTS5* and *EPAS1*), anabolic (*COL2A1* and *ACAN*) and hypertrophic markers (*COL1A1*, *COL10A1* and *ALPL*). As shown in **Figure 1**, non-beneficial chondrocyte responses to 65%MS were particularly marked by increased expression of *MMP13* (FC=6.61; *P*-value=5.17x10$^{-5}$, **Figure 1E**) and *EPAS1* (FC=1.79; *P*-value=5.49x10$^{-6}$), and reduced expression of *COL2A1* (FC=0.49; *P*-value=3.43x10$^{-3}$, **Figure 1F**) and *ACAN* (FC=0.75; *P*-value=1.79x10$^{-2}$; **Table 1**).

Next, to investigate if attenuation of thyroid signalling is a promising treatment for OA, osteochondral explants subjected to 65%MS were simultaneously treated with the anti-deiodinase IOP. As shown in **Table 1**, upon administration of IOP to samples subjected to 65%MS, catabolic markers *MMP13* (FC=0.10; *P*-value=1.73x10$^{-4}$) and *ADAMTS5* (FC=0.43; *P*-value=2.16x10$^{-2}$) were downregulated compared to 65%MS. In addition, expression of the anabolic marker *COL2A1* (FC=3.58; *P*-value=3.71x10$^{-5}$; **Figure 1F**) was no longer downregulated by 65%MS after IOP treatment. For hypertrophic markers, *COL10A1* (FC=0.23; *P*-value=1.05x10$^{-3}$) was significantly downregulated after IOP treatment, while downregulation of *COL1A1* (FC=0.11; *P*-value=5.29x10$^{-2}$) and *ALPL* (FC=0.03; *P*-val ue=5.71x10$^{-2}$) did not reach statistical significance. With respect to catabolic marker *EPAS1*, no restoration or beneficial effects of IOP treatment with 65%MS was observed.

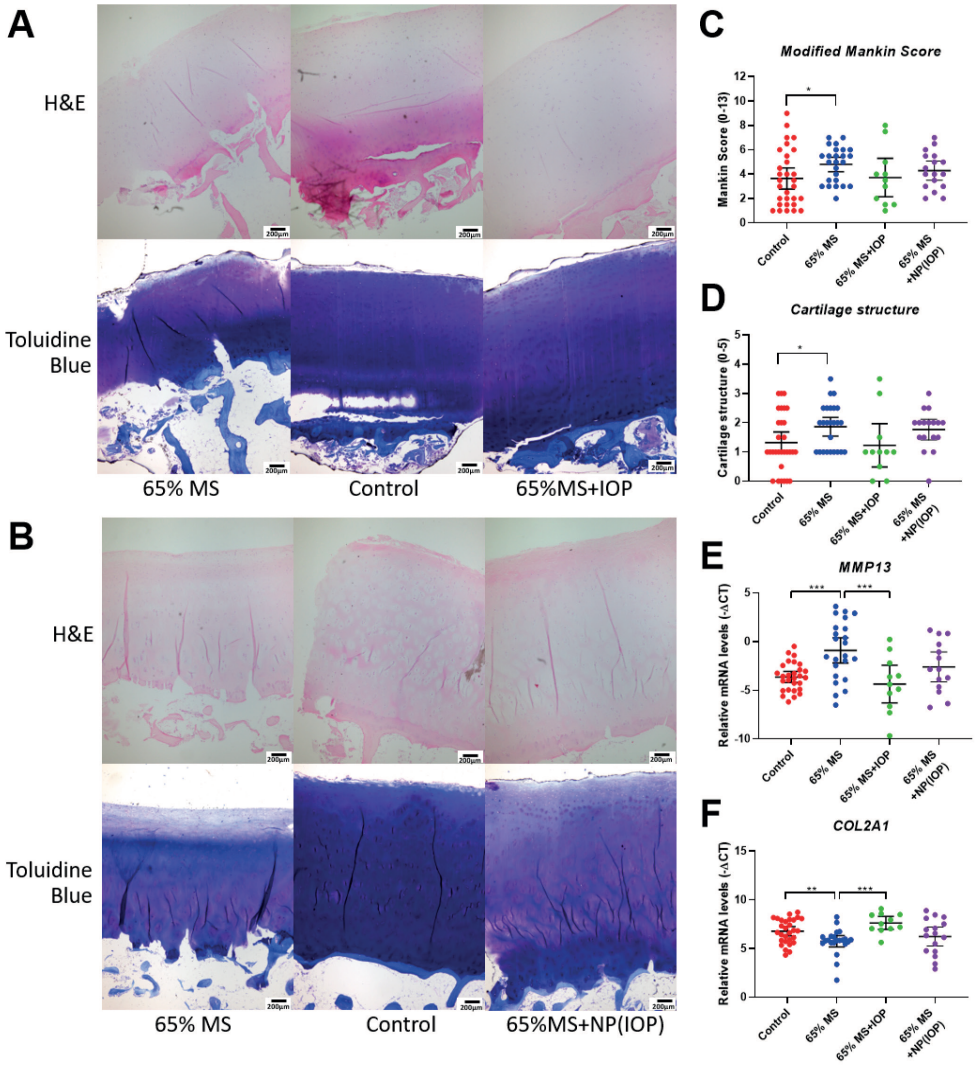



**Figure 1 | Mankin score and gene expression of human aged osteochondral explants after treatment with IOP. [A, B]** Representative histological pictures of Toluidine blue and H&E stainings. **[C]** Cartilage damage was assessed by determining the Mankin score with **[D]** scoring of cartilage structure. RT-PCR analysis of **[E]** *MMP13* and **[F]** *COL2A1*. Data is presented as scatter dot plots, with mean and 95%CI, and each dot represents a sample. P-values of mean differences between controls and treated explants were estimated by generalized estimating equations (GEE) with expression or Mankin score as dependent variable, treatment as factor and robust variance estimators to account for donor effects. Legend: H&E=haematoxylin and eosin; 65%MS=65% mechanical stress; IOP=iopanoic acid; NP=nanoparticle. *P<0.05, **P<0.01, ***P<0.001.

As a proof of concept and to determine wether IOP delivery from PLGA-PEG NP(IOP) is effective, chondrocyte signalling was measured in response to 65%MS now with PLGA NP(IOP) treatment. Upon administration of PLGA NP(IOP), decreased expression of *MMP13* in comparison with 65%MS as control was observed (FC=0.38; *P*-value=9.53x10$^{-2}$; **Figure 1** and **Table 1**), albeit less pronounced and not significant. On the other hand, upon comparing

the 65%MS with NP(IOP) group to unperturbed controls, changes in *MMP13* and *COL2A1* expression were no longer significant (**Figure 1E-F** and **Supplementary Table S3**). For the hypertrophic markers, no changes were measured in cartilage treated with PLGA NP(IOP) receiving 65%MS. To conclude, IOP encapsulated in PLGA NPs appear to prevent unbeneficial gene expression changes induced by 65%MS, although effectiveness when compared with repeated treatment with free IOP is less pronounced.

**Table 1 | Summary of outcome parameters in response to the different perturbations.**

| **Outcome measure** | **control vs 65%MS** | | **65%MS vs 65%MS+IOP** | | **65%MS vs 65%MS+NP(IOP)** | |
|---|---|---|---|---|---|---|
| | **FC[&]** | ***P*-value[$]** | **FC[&]** | ***P*-value[$]** | **FC[&]** | ***P*-value[$]** |
| Gene expression | | | | | | |
| Catabolism | | | | | | |
| *MMP13* | 6.44 | $5.17x10^{-5}$ | 0.10 | $1.73x10^{-4}$ | 0.38 | $9.53x10^{-2}$ |
| *ADAMTS5* | 0.90 | NS | 0.43 | $2.16x10^{-2}$ | 0.85 | NS |
| *EPAS1* | 1.79 | $5.49x10^{-6}$ | 1.32 | NS | 1.21 | $9.29x10^{-2}$ |
| Anabolism | | | | | | |
| *ACAN* | 0.66 | $1.79x10^{-2}$ | 1.29 | NS | 1.18 | NS |
| *COL2A1* | 0.40 | $3.43x10^{-3}$ | 3.58 | $3.71x10^{-5}$ | 1.68 | NS |
| Hyperthrophy | | | | | | |
| *COL1A1* | 1.03 | NS | 0.11 | $5.29x10^{-2}$ | 0.56 | NS |
| *COL10A1* | 1.81 | NS | 0.23 | $1.05x10^{-3}$ | 0.93 | NS |
| *ALPL* | 1.27 | NS | 0.03 | $5.71x10^{-2}$ | 0.54 | NS |
| **Outcome Measure** | **control vs 65%MS** | | **65%MS vs 65%MS+IOP** | | **65%MS vs 65%MS+NP(IOP)** | |
| | **Beta[+]** | ***P*-value[$]** | **Beta[+]** | ***P*-value[$]** | **Beta[+]** | ***P*-value[$]** |
| Histology | | | | | | |
| Mankin score | 1.15 | $2.30x10^{-2}$ | -0.83 | NS | -0.61 | NS |
| *Cartilage structure* | 0.54 | $1.90x10^{-2}$ | -0.48 | NS | -0.16 | NS |
| *Cellularity* | 0.25 | NS | 0.12 | NS | -0.21 | NS |
| *Toluidine blue* | 0.34 | NS | -0.42 | NS | -0.21 | NS |
| *Tidemark integrity* | 0.14 | NS | -0.14 | NS | -0.17 | NS |
| sGAG | | | | | | |
| Medium | 33.68 | $1.58x10^{-2}$ | -19.81 | NS | -3.94 | NS |

The comparisons outlined in the table are mechanical stress (65%MS) compared to unperturbed controls, injurious mechanicals stress treated with IOP (65%MS+IOP) compared to 65%MS and injurious mechanicals stress treated with PLGA nanoparticles filled with IOP (65%MS+NP(IOP)) compared to 65%MS. [&]FC is determined by the $2^{-\Delta\Delta CT}$ method and compared to its respective control. [+]Beta is determined by the GEE during modelling. [$]Significance of mean difference in parameters between explant treatment groups were estimated by generalized estimating equation (GEE) with robust variance estimators to account for donor effects. Legend: FC=fold change; MS=Mechanical stress; IOP=iopanoic acid; NP=nanoparticle; NS=not significant; sGAG=sulphated glycosaminoglycans.

### *IOP reduces cartilage integrity changes in aged human osteochondral explants*

Next, we explored whether the gene expression changes translate to changes in the histological Mankin scores. As shown in **Figure 1A** and **Figure 1B,** an increased Mankin score among 65%MS explants as compared with controls (4.80±0.29 versus 3.65±0.43; *P*-value=$2.34x10^{-2}$; **Figure 1C**) confirmed damage. More specifically, increased Mankin score was particularly due to increased cartilage structure damage score (1.86±0.15 versus 1.32±0.18; *P*-value=$1.94x10^{-2}$;

**Figure 1D**). Upon investigating explants subjected to 65%MS with IOP or PLGA NP(IOP) we observed Mankin scores comparable to controls (3.72±0.71 and 4.29±0.37; **Figure 1D, Supplementary Table S3**). In line with this, sGAG released from 65%MS osteochondral explants was increased by 49% compared with controls (91.85±13.00 μg/ml versus 61.45±5.11 μg/ml; *P*-value=1.58x10$^{-2}$; **Table 1**). Whereas after free IOP treatment, 65%MS induced no change in sGAG release in comparison to controls (61.68±9.13 μg/ml versus 61.45±5.11 μg/ml; **Supplementary Table S3**). PLGA NP(IOP) treatment did not reduce sGAG release to the media with 65%MS (95.91±14.32 μg/ml versus 61.45±5.11 μg/ml; *P*-value=4.07x10$^{-2}$; **Supplementary Table S3**).

### *RNA-sequencing of IOP treated explants upon applying 65%MS*

To investigate the mode of action of IOP on injurious mechanical stress induced changes, genome-wide gene expression was measured by sequencing RNA of explant cartilage treated with free IOP and 65%MS ($n_{65\%MS+IOP}$=7) and compared them with the 65%MS group as control ($n_{65\%MS}$=14), as such identifying genes that sequester the damaging response upon injurious loading.

Prior to genome wide analysis, we confirmed expression changes of genes previously measure by RT-qPCR in our osteochondral explant model (**Table 1**). As shown in **Supplementary Table S4**, RNA-sequencing replicated downregulated expression of *MMP13* (FC=0.06; *P*-value=9.00x10$^{-3}$) and of hypertrophic markers *COL1A1* (FC=0.02; *P*-value=4.72x10$^{-4}$) and *ALPL* (FC=0.01; *P*-value=3.65x10$^{-3}$) in 65%MS+IOP cartilage when compared to 65%MS cartilage. For *COL10A1* (FC=0.18; *P*-value=6.36x10$^{-2}$) reduced expression was observed in the RNA-sequencing, but did not reach statistical significance. Moreover, despite the similar effect sizes of *COL2A1* in RT-qPCR and RNA-sequencing, these effects were not significant in the latter.

**Table 2 | The 12 FDR significantly differentially expressed genes between IOP and 65% MS cartilage.**

| Gene | FC | *P*-value | FDR[a] |
|---|---|---|---|
| *INSIG1* | 3.25 | 6.12x10$^{-6}$ | 2.24x10$^{-2}$ |
| *DHCR7* | 2.92 | 1.47x10$^{-5}$ | 3.28x10$^{-2}$ |
| *FADS1* | 2.91 | 1.88x10$^{-5}$ | 3.28x10$^{-2}$ |
| *LRP8* | 2.87 | 3.75x10$^{-5}$ | 4.58x10$^{-2}$ |
| *ACAT2* | 2.25 | 1.55x10$^{-5}$ | 3.28x10$^{-2}$ |
| *LTBP2* | 0.43 | 2.01x10$^{-5}$ | 3.28x10$^{-2}$ |
| *CTGF* | 0.35 | 3.78x10$^{-6}$ | 2.24x10$^{-2}$ |
| *BMP5* | 0.29 | 2.47x10$^{-5}$ | 3.29x10$^{-2}$ |
| *LOX* | 0.23 | 4.14x10$^{-6}$ | 2.24x10$^{-2}$ |
| *ADGRV1* | 0.21 | 4.66x10$^{-6}$ | 2.24x10$^{-2}$ |
| *FOXM1* | 0.16 | 1.74x10$^{-5}$ | 3.28x10$^{-2}$ |
| *MASP1* | 0.13 | 2.27x10$^{-5}$ | 3.29x10$^{-2}$ |

[a] To correct for multiple testing, the Benjamini-Hochberg method was applied to *P*-values and reported as the false discovery rate (FDR). Legend: FC=fold change; FDR=False discovery rate

Next, genome wide differential expression analysis with 65%MS as control versus 65%MS+IOP was performed, indicating 12 FDR significant differentially expressed (DEGs; **Table 2).** Of these 12 DEGs, five were upregulated while seven were downregulated with absolute fold changes ranging from 2.25 to 7.69. The highest upregulated gene was *INSIG1* (FC=3.25; FDR=$2.24x10^{-2}$), encoding for insulin induced gene 1, a protein inhibiting lipogenesis and cell proliferation [20]. The most downregulated gene was *MASP1* (FC=0.13; FDR=$3.29x10^{-2}$), encoding for mannan binding lectin serine peptidase 1, a serine protease involved in complement activation [21]. Of interest is also the identification of downregulated genes promoting chondrocyte proliferation and differentiation such as *BMP5* (FC=0.29; FDR=$3.29x10^{-2}$), encoding for bone morphogenetic protein 5, and *CTGF* (FC=0.35; FDR=$2.24x10^{-2}$), encoding connective tissue growth factor [22,23].

Protein-protein interactions of the DEGs were investigated in STRING and showed significantly more interactions than expected by chance (*P*-value=$2.61x10^{-7}$), with 7 out of 12 proteins having connections (**Figure 2**). Of note is that connected proteins (*INSIG1*, *DHCR7*, *FADS1* and *ACAT2*) consists of those involved in cholesterol biosynthetic processes (GO:0006695). To conclude, treatment with IOP shows changes in gene expression patterns that suggest a response in metabolic processes (*INSIG1*, *DHCR7*, *FADS1* and *ACAT2*) and reduction of proliferation and differentiation (*CTGF*, *BMP5* and *FOXM1*) in chondrocytes.

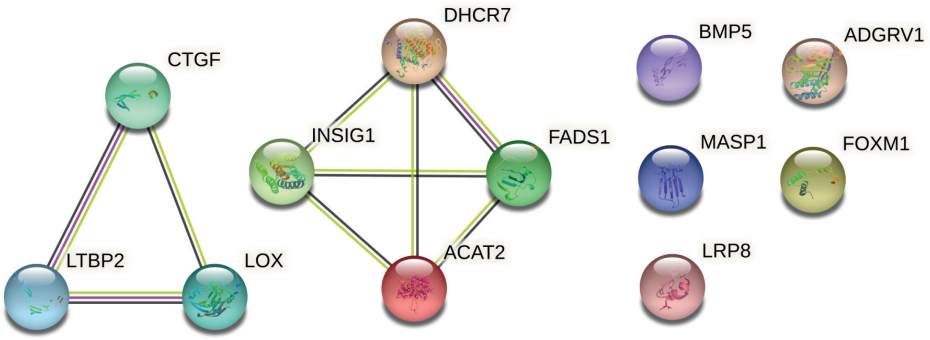



**Figure 2 | Protein-Protein interaction network in STRING of proteins encoded by differentially expressed genes.** Differentially expressed genes between 65%MS and 65%MS+IOP cartilage of osteochondral explants show two connected gene groups with high interactions

### *Comparison between IOP responsive and OA responsive genes.*

To investigate to what extend the DEGs coincide with OA pathophysiology, we compared DEGs ($DEG_{IOP}$) with previously identified DEGs between preserved and lesioned OA cartilage ($DEG_{OA}$) [4]. Of the 12 DEGs, three were also involved in OA pathophysiology (**Table 3**). Notable are *ADGRV15726*, encoding for the calcium binding transmembrane receptor adhesion g protein-coupled receptor V1, and *FOXM1*, encoding for the transcription factor forkhead box protein M1, a known inducer of cell proliferation and key mediator of inflammatory signalling [24], since they mark OA pathophysiology [4] and are being counteracted by IOP treatment (**Table 3**). *DHCR7*, a vital enzyme for cholesterol and vitamin D production [25], was upregulated in both OA pathophysiology and in response to IOP treatment. In addition, we investigated if any of the here identified DEGs are also seen as OA susceptibility risk genes and identified that for *BMP5* several polymorphisms have been associated with OA [26,27].

**Table 3 | Investigation of the 12 FDR significant genes in OA pathophysiology.**

| | 65%MS+IOP vs 65%MS | | | OA pathophysiology[b] | | |
|---|---|---|---|---|---|---|
| **Gene** | **FC** | ***P*-value** | **FDR[a]** | **FC** | ***P*-value** | **FDR[a]** |
| ***INSIG1*** | 3.25 | $6.12x10^{-6}$ | $2.24x10^{-2}$ | 1.04 | NS | NS |
| ***DHCR7*** | 2.92 | $1.47x10^{-5}$ | $3.28x10^{-2}$ | 1.28 | $1.21x10^{-3}$ | $1.56x10^{-2}$ |
| ***FADS1*** | 2.91 | $1.88x10^{-5}$ | $3.28x10^{-2}$ | 1.00 | NS | NS |
| ***LRP8*** | 2.87 | $3.75x10^{-5}$ | $4.58x10^{-2}$ | 1.15 | $3.00x10^{-2}$ | NS |
| ***ACAT2*** | 2.25 | $1.55x10^{-5}$ | $3.28x10^{-2}$ | 1.19 | $3.00x10^{-2}$ | NS |
| ***LTBP2*** | 0.43 | $2.01x10^{-5}$ | $3.28x10^{-2}$ | 1.06 | NS | NS |
| ***CTGF*** | 0.35 | $3.78x10^{-6}$ | $2.24x10^{-2}$ | 1.18 | $1.00x10^{-2}$ | NS |
| ***BMP5*** | 0.29 | $2.47x10^{-5}$ | $3.29x10^{-2}$ | 0.74 | NS | NS |
| ***LOX*** | 0.23 | $4.14x10^{-6}$ | $2.24x10^{-2}$ | 1.13 | NS | NS |
| ***ADGRV1*** | 0.21 | $4.66x10^{-6}$ | $2.24x10^{-2}$ | 1.72 | $2.87x10^{-3}$ | 2.92x1°-2 |
| ***FOXM1*** | 0.16 | $1.74x10^{-5}$ | $3.28x10^{-2}$ | 1.40 | $2.31x10^{-3}$ | $2.50x10^{-2}$ |
| ***MASP1*** | 0.13 | $2.27x10^{-5}$ | $3.29x10^{-2}$ | 0.89 | NS | NS |

[a] To correct for multiple testing, the Benjamini-Hochberg method was applied to *P*-values and reported as the false discovery rate (FDR). [b]Gene expression changes measured in RNA-sequencing data between preserved and lesioned OA articular cartilage, with preserved as reference [4]. Legend: FC=fold change; FDR=false discovery rate; OA=osteoarthritis; 65%MS=65% mechanical stress; NS=not significant; IOP=iopanoic acid.



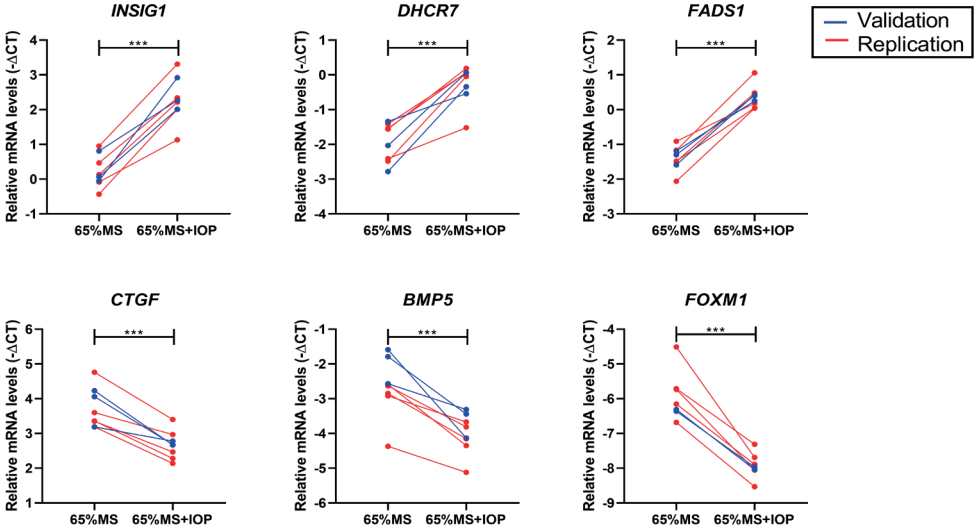



**Figure 3 | Technical and biological validation of the highest up- and downregulated genes was performed using RT-qPCR.** Expression of three upregulated (*INSIG1*, *DHCR7*, *FADS1*) and three downregulated (*CTGF*, *BMP5*, *FOXM1*) genes was validated (blue; n=3 pairs) and replicated (red; n=5 pairs) in cartilage samples by RT-qPCR. Figures show connected paired samples and -ΔCT of each independent sample is depicted by black dots in the graphs. Statistical differences between gene expression in 65%MS and IOP treated 65%MS cartilage (65%MS+IOP) was determined with a linear generalized estimation equation (GEE) with mRNA level as dependent variable.***P≤0.001. Legend: 65%MS: 65% mechanical stress; RT-qPCR: reverse transcriptase-quantitative PCR; IOP=iopanoic acid.

### *Validation of DEGs*

For technical validation (n=3 pairs) and biological replication (n=5 pairs) of the DEGs identified in this study, RT-qPCR was performed for three upregulated (*INSIG1*, *DHCR7*, *FADS1*) and three downregulated (*CTGF*, *BMP5*, *FOXM1*) genes. For all genes a significant difference was confirmed between 65%MS and 65%MS+IOP treated cartilage (**Figure 3**), with the same direction and size of effects, confirming robustness of our RNA sequencing results.

## Discussion

In the current study we explored possible beneficial effects of inhibiting D2 activity by adding the anti-deiodinase agent IOP to our previously established aged human osteochondral explant model. Herein detrimental effects were initiated by the OA-relevant trigger injurious mechanical stress (65%MS) [15]. To allow further translation of our results we additionally studied effects of prolonged IOP release from nanoparticles. Our results confirmed that treatment with IOP reduced the majority of detrimental 65%MS-induced chondrocyte signalling and even reduced some of its long-term effects on cartilage integrity. Finally, RNA-sequencing was performed on 65%MS cartilage with and without IOP treatment, which enable us to identify its mode of action.

We identified 12 DEGs of which the majority are involved in metabolic processes (e.g. *INSIG1*, *DHCR7*, *FADS2* and *ACAT2*) and cell proliferation and differentiation (e.g. *CTGF*, *BMP5* and *FOXM1*), indicating IOP is reducing metabolic activity of chondrocytes possibly towards a healthy resting state. This is in line with previous studies showing that adult chondrocytes and the extracellular cartilage matrix benefitted from maintaining a low metabolic maturation-arrested state, while activation of aged chondrocytes results in proliferation, recapitulation of endochondral ossification and eventually cell death [4,28].

We here show that treatment with free IOP in the medium efficiently reduced cartilage degradation of human aged osteochondral explants subjected to injurious mechanical stress. These effects were however less pronounced when we administered PLGA NP(IOP). A possible explanation for the reduced effectiveness of IOP released from NPs, could be that the pharmacological agent is not released in a high enough doses to counteract the detrimental induction. This is further exacerbated by the fact that IOP released slowly from the NP is subjected to a half-life of 1-2 days [29], whereas IOP in the medium was refreshed every 3-4 days. On the other hand, the relatively low concentration of 10 μM encapsulated IOP was based on pilot experiments and the underlying thought that NP are being taken up by chondrocytes (**Supplementary Fig 2A**), and thus acting locally and more efficiently. In any case, given that PLGA NP(IOP) appeared less effective, the exact concentration of PLGA NP(IOP) requires further optimization. Moreover, delivery of the NPs can be further optimized, e.g. by modifying charge of the NP to increase retention in the synovial cavity or binding to negatively charged sGAGs. Other factors that need to be considered before performing *in vivo* studies are the effects of tissue disease state, synovial fluid, and NP accumulation as these may modify retention, delivery efficiency and drug efficacy.

To investigate the mode of action of IOP, transcriptome-wide differences between cartilage of osteochondral explants subjected to injurious mechanical stress with and without IOP was determined showing 12 FDR significant genes with suggested high protein-protein

connectivity (**Figure 2**). Notably, these genes appeared to be primarily involved in metabolic processes, such as *INSIG1* (FC=3.25; FDR=$2.24x10^{-2}$) encoding a membrane protein that limits lipogenesis and cell differentiation [20]. Another notable gene in this respect was *BMP5* (FC=0.29; FDR=$3.29x10^{-2}$). BMP5 is a ligand of the TGF-beta superfamily involved in activation of SMAD, ERK and p38 induced gene expression, negatively affecting cartilage homeostasis [30]. On the other hand, *BMP5* silencing reduced OA progression in mice [31]. Together these data suggest that IOP may have reduced detrimental effects of injurious mechanical stress via lowering BMP5 activation. Of interest is the identification of the transcription factor, *FOXM1* (FC=0.16; FDR=$1.74x10^{-5}$), coinciding with genes involved in OA pathophysiology (**Table 3**) and a key mediator of the inflammatory response inducing OA degeneration [24]. The herein observed downregulation of *FOXM1* suggests that IOP could protect chondrocytes from an inflammatory response upon external stimuli. Finally, because IOP is an inhibitor of thyroid signalling, we compared the 12 DEGs to a consensome meta-analysis of thyroid manipulation studies [32]. Nine (75%) genes were confirmed to be involved in thyroid signalling and among them we identified important genes such as *INSIG1*, *DHCR7*, *FADS1* and *ACAT2* involved in the metabolic process of cholesterol biosynthetic processes (**Supplementary Table S5**). To conclude, genome-wide changes of IOP show its ability to reduce the metabolic activity of chondrocytes as observed by the response of genes involved in metabolic processes and cell proliferation and differentiation.



Although the model used in our study is prone to OA pathophysiology, as it consists of physiologically relevant human aged preserved articular cartilage and subchondral bone, the model is inherently subject to heterogeneity. Nonetheless, in general our results were robustly reflected in multiple donors, giving validity to the observed effects. The RNA-sequencing was performed in a low number of samples, resulting in limited power to identify DEGs with a lower effect. However, by comparing RT-qPCR results with the RNA-sequencing results we show the validity of the results of the RNA-sequencing, as observed by similar effect sizes and *P*-values. Altogether, by combining treatment testing of a genetically based (repurposed) drug in an established human aged biomimetic osteochondral explant model of mechanical injury [15,33], we generated multiple reliable biological replicates on how abrogation of thyroid signalling in cartilage is beneficial for cartilage homeostasis. As such, our approach created reliable data that are highly translatable to the *in vivo* human situation while contributing to the societal need for animal study reduction. In this study we focussed on measuring chondrocyte signalling on the gene expression level since thyroid hormone primarily affects metabolic processes via binding to the thyroid receptor, which regulates downstream gene expression. Additionally, we believe gene expression to be a measurement reflecting detrimental chondrocyte homeostasis prior to any detrimental effects observed in the extracellular matrix.

In this study, we have shown that treatment with the anti-deiodinase IOP reduced detrimental changes induced by injurious mechanical stress. In addition, by performing RNA-sequencing we identified that its mode of action mainly encompassed metabolic processes, cell proliferation and differentiation and also important OA-associated genes, such as *BMP5*, *CTGF* and *FOXM1*. Since in general a lower metabolism has been shown to be beneficial for chondrocytes, we advocate use of IOP is a potential pharmacological treatment agent for OA.

### *Funding*

This work was supported by the Dutch Scientific Research council NWO/ZonMW VICI scheme (nr 91816631/528) and the Dutch Arthritis Society/ReumaNederland (15-4-401).

### *Acknowledgments*

We thank all the participants of the RAAK study. The LUMC has and is supporting the RAAK study. We also thank Enrike van der Linden, Robert van der Wal, Peter van Schie, Anika Rabelink-Hoogenstraaten, Shaho Hasan, Maartje Meijer, Daisy Latijnhouwers and Geert Spierenburg for collecting surgical waste material. Data is generated within the scope of the Medical Delta Programs Regenerative Medicine 4D: Generating complex tissues with stem cells and printing technology and Improving Mobility with Technology.

### *Competing interest*

The authors declare that they have no competing interests.

### *Ethics*

Our study complies with the Declaration of Helsinki. Furthermore, the RAAK study has been approved by the medical ethical committee of the Leiden University Medical Center (P08.239/P19.013) and informed consent was obtained from subjects.

### *Data availability statement*

Data are available on reasonable request. RNA sequencing data underlying this article are available in the European Genome-phenome Archive (EGA) at https://ega-archive.org/ and can be accessed with EGAS00001006242.

## REFERENCES

1. Bijlsma JW, Berenbaum F, Lafeber FP. Osteoarthritis: an update with relevance for clinical practice. *Lancet*. 2011;377(9783):2115-26.
2. Drissi H, Zuscik M, Rosier R, et al. Transcriptional regulation of chondrocyte maturation: potential involvement of transcription factors in OA pathogenesis. *Mol Aspects Med*. 2005;26(3):169-79.
3. Felson DT. Developments in the clinical understanding of osteoarthritis. *Arthritis Res Ther*. 2009;11(1):203.
4. Coutinho de Almeida R, Ramos YFM, Mahfouz A, et al. RNA sequencing data integration reveals an miRNA interactome of osteoarthritis cartilage. *Annals of the rheumatic diseases*. 2019;78(2):270-7.
5. den Hollander W, Ramos YF, Bomer N, et al. Transcriptional associations of osteoarthritis-mediated loss of epigenetic control in articular cartilage. *Arthritis & rheumatology (Hoboken, NJ)*. 2015;67(8):2108-16.

6. Nelson MR, Tipney H, Painter JL, et al. The support of human genetic evidence for approved drug indications. *Nat Genet*. 2015;47(8):856-60.
7. Meulenbelt I, Min JL, Bos S, et al. Identification of DIO2 as a new susceptibility locus for symptomatic osteoarthritis. *Hum Mol Genet*. 2008;17(12):1867-75.
8. Gereben B, Zavacki AM, Ribich S, et al. Cellular and molecular basis of deiodinase-regulated thyroid hormone signaling. *Endocr Rev*. 2008;29(7):898-938.
9. Bos SD, Bovee JV, Duijnisveld BJ, et al. Increased type II deiodinase protein in OA-affected cartilage and allelic imbalance of OA risk polymorphism rs225014 at DIO2 in human OA joint tissues. *Annals of the rheumatic diseases*. 2012;71(7):1254-8.
10. Ijiri K, Zerbini LF, Peng H, et al. Differential expression of GADD45beta in normal and osteoarthritic cartilage: potential role in homeostasis of articular chondrocytes. *Arthritis Rheum*. 2008;58(7):2075-87.
11. Bomer N, Cornelis FM, Ramos YF, et al. The effect of forced exercise on knee joints in Dio2(-/-) mice: type II iodothyronine deiodinase-deficient mice are less prone to develop OA-like cartilage damage upon excessive mechanical stress. *Annals of the rheumatic diseases*. 2016;75(3):571-7.
12. Bomer N, den Hollander W, Ramos YF, et al. Underlying molecular mechanisms of DIO2 susceptibility in symptomatic osteoarthritis. *Annals of the rheumatic diseases*. 2015;74(8):1571-9.
13. Nagase H, Nagasawa Y, Tachida Y, et al. Deiodinase 2 upregulation demonstrated in osteoarthritis patients cartilage causes cartilage destruction in tissue-specific transgenic rats. *Osteoarthritis and cartilage*. 2013;21(3):514-23.
14. Tyer NM, Kim TY, Martinez DS. Review of Oral Cholecystographic Agents for the Management of Hyperthyroidism. *Endocr Pract*. 2014;20(10):1084-92.
15. Houtman E, van Hoolwerff M, Lakenberg N, et al. Human Osteochondral Explants: Reliable Biomimetic Models to Investigate Disease Mechanisms and Develop Personalized Treatments for Osteoarthritis. *Rheumatol Ther*. 2021;8(1):499-515.
16. Ramos YF, den Hollander W, Bovee JV, et al. Genes involved in the osteoarthritis process identified through genome wide expression analysis in articular cartilage; the RAAK study. *PLoS One*. 2014;9(7):e103056.
17. Love MI, Huber W, Anders S. Moderated estimation of fold change and dispersion for RNA-seq data with DESeq2. *Genome Biol*. 2014;15(12):550.
18. Szklarczyk D, Gable AL, Lyon D, et al. STRING v11: protein-protein association networks with increased coverage, supporting functional discovery in genome-wide experimental datasets. *Nucleic Acids Res*. 2019;47(D1):D607-D13.
19. Diggle P, Liang K-Y, Zeger SL. Analysis of longitudinal data. Oxford New York: Clarendon Press; Oxford University Press; 1994. xi, 253 p. p.
20. 20. Li J, Takaishi K, Cook W, et al. Insig-1 "brakes" lipogenesis in adipocytes and inhibits differentiation of preadipocytes. *Proc Natl Acad Sci U S A*. 2003;100(16):9476-81.21.
21. Degn SE, Jensen L, Hansen AG, et al. Mannan-binding lectin-associated serine protease (MASP)-1 is crucial for lectin pathway activation in human serum, whereas neither MASP-1 nor MASP-3 is required for alternative pathway function. *J Immunol*. 2012;189(8):3957-69.
22. Mailhot G, Yang M, Mason-Savas A, et al. BMP-5 expression increases during chondrocyte differentiation in vivo and in vitro and promotes proliferation and cartilage matrix synthesis in primary chondrocyte cultures. *J Cell Physiol*. 2008;214(1):56-64.
23. Ivkovic S, Yoon BS, Popoff SN, et al. Connective tissue growth factor coordinates chondrogenesis and angiogenesis during skeletal development. *Development*. 2003;130(12):2779-91.
24. Zeng RM, Lu XH, Lin J, et al. Knockdown of FOXM1 attenuates inflammatory response in human osteoarthritis chondrocytes. *Int Immunopharmacol*. 2019;68:74-80.
25. Prabhu AV, Luu W, Li D, et al. DHCR7: A vital enzyme switch between cholesterol and vitamin D production. *Prog Lipid Res*. 2016;64:138-51.
26. Southam L, Dowling B, Ferreira A, et al. Microsatellite association mapping of a primary osteoarthritis susceptibility locus on chromosome 6p12.3-q13. *Arthritis Rheum*. 2004;50(12):3910-4.
27. Tachmazidou I, Hatzikotoulas K, Southam L, et al. Identification of new therapeutic targets for osteoarthritis through genome-wide analyses of UK Biobank data. *Nat Genet*. 2019;51(2):230-6.

28. Sandell LJ, Aigner T. Articular cartilage and changes in arthritis. An introduction: cell biology of osteoarthritis. *Arthritis Res*. 2001;3(2):107-13.
29. Eason CT, Frampton CM. The plasma pharmacokinetics of iophenoxic and iopanoic acids in goat. *Xenobiotica*. 1992;22(2):185-9.
30. Snelling SJ, Hulley PA, Loughlin J. BMP5 activates multiple signaling pathways and promotes chondrogenic differentiation in the ATDC5 growth plate model. *Growth Factors*. 2010;28(4):268-79.
31. Shao Y, Zhao C, Pan J, et al. BMP5 silencing inhibits chondrocyte senescence and apoptosis as well as osteoarthritis progression in mice. *Aging (Albany NY)*. 2021;13(7):9646-64.
32. Ochsner SA, McKenna NJ. No Dataset Left Behind: Mechanistic Insights into Thyroid Receptor Signaling Through Transcriptomic Consensome Meta-Analysis. *Thyroid*. 2020;30(4):621-39.
33. Houtman E, Tuerlings M, Riechelman J, et al. Elucidating mechano-pathology of osteoarthritis: transcriptome-wide differences in mechanically stressed aged human cartilage explants. *Arthritis Res Ther*. 2021;23(1):215.

# Supplementary Files

## *List of content:*

### *Supplementary Tables*

**Supplementary Table S1.** Baseline information of the donors included in this study.

**Supplementary Table S2**. Primer sequences used in RT-qPCR.

**Supplementary Table S3.** Summary of the different outcome parameters in response to perturbation with 65% mechanical stress (65%MS), 65%MS+IOP and 65%MS+PLGA NP(IOP) compared to unperturbed controls.

**Supplementary Table S4.** Gene expression measured by RT-qPCR and RNA sequencing between 65%MS+IOP in comparison to 65%MS.

**Supplementary Table S5.** Investigation of the 12 FDR significant genes in a consensome of thyroid signalling.



### *Supplementary Materials and Methods*

### *Supplementary Figures*

**Supplementary Figure S1.** Schematic representation of study setup.

**Supplementary Figure S2.** Characterization of PLGA-PEG nanoparticles.

# Supplementary Tables

**Supplementary Table S1 | Baseline information of the donors included in this study.**

| Characteristic | Average±SD [Range] |
|---|---|
| Age | 67.1±9.8 [52-85] |
| Sex | 4M, 12F (75% F) |
| BMI | 30.8±4.7 [24.6-39.2] |

The table represents the age, sex, and BMI of donors used in this study. Legend: F=Females, M=Males; age given in years)

**Supplementary Table S2 | Primer sequences used in RT-qPCR.**

| Gene | Forward primer (5'- 3') | Reverse primer (5'- 3') |
|---|---|---|
| *SDHA* | TGGAGCTGCAGAACCTGATG | TGTAGTCTTCCCTGGCATGC |
| *YWHAZ* | CTGAGGTTGCAGCTGGTGATGACA | AGCAGGCTTTCTCAGGGGAGTTCA |
| *MMP13* | TTGAGCTGGACTCATTGTCG | GGAGCCTCTCAGTCATGGAG |
| *ADAMTS5* | TGGCTCACGAAATCGGACAT | GCGCTTATCTTCTGTGGAACC |
| *EPAS1* | ACAGGTGGAGCTAACAGGAC | CCGTGCACTTCATCCTCATG |
| *COL2A1* | CTACCCCAATCCAGCAAACGT | AGGTGATGTTCTGGGAGCCTT |
| *ACAN* | AGAGACTCACACAGTCGAAACAGC | CTATGTTACAGTGCTCGCCAGTG |
| *COL1A1* | GTGCTAAAGGTGCCAATGGT | ACCAGGTTCACCGCTGTTAC |
| *COL10A1* | GGCAACAGCATTATGACCCA | TGAGATCGATGATGGCACTCC |
| *ALPL* | CAAAGGCTTCTTCTTGCTGGTG | CCTGCTTGGCTTTTCCTTCA |
| *INSIG1* | GCTGCAGATCCAGAGGAATGT | GTGACTGTCGATACAGGGGT |
| *DHCR7* | ACAGAACCGCATCTCAAGGG | AGCTGTACTGGTCACAAGCC |
| *FADS1* | AGCTTTGAGCCCACCAAGAA | CATCCAGCAGCAAGATGTGC |
| *CTGF* | CCGTACTCCCAAAATCTCCA | ATGTCTTCATGCTGGTGCAG |
| *BMP5* | ACTCTATGTGAGCTTCCGGG | CAGCGTATCCTTCTGGTGCT |
| *FOXM1* | TCACAGCAGAAACGACCGAA | TCACCGGGAACTGGATAGGT |

**Supplementary Table S3 | Summary of the different outcome parameters in response to perturbation with 65% mechanical stress (65%MS), 65%MS+IOP and 65%MS+PLGA NP(IOP) compared to unperturbed controls.**

| **Outcome measure** | **65%MS+IOP vs control** | | **65%MS+NP(IOP) vs control** | |
|---|---|---|---|---|
| | **FC[a]** | ***P*-value[$]** | **FC[a]** | ***P*-value[$]** |
| Gene expression | | | | |
| Catabolism | | | | |
| *MMP13* | 0.60 | NS | 2.05 | NS |
| *ADAMTS5* | 0.12 | $1.99x10^{-2}$ | 1.05 | NS |
| *EPAS1* | 2.06 | $1.71x10^{-3}$ | 2.11 | $1.17x10^{-9}$ |
| Anabolism | | | | |
| *ACAN* | 0.68 | NS | 0.99 | NS |
| *COL2A1* | 1.79 | NS | 0.85 | NS |
| Hyperthrophy | | | | |
| *COL1A1* | 0.14 | $4.02x10^{-2}$ | 0.48 | NS |
| *COL10A1* | 0.22 | $3.06x10^{-2}$ | 1.55 | NS |
| *ALPL* | 0.11 | $6.20x10^{-2}$ | 0.53 | NS |
| **Outcome Measure** | **65%MS+IOP vs control** | | **65%MS+NP(IOP) vs control** | |
| | **Beta[b]** | ***P*-value[$]** | **Beta[b]** | ***P*-value[$]** |
| Histology | | | | |
| Mankin score | 0.32 | NS | 0.55 | NS |
| *Cartilage structure* | 0.07 | NS | 0.39 | NS |
| *Cellularity* | 0.37 | NS | 0.04 | NS |
| *Toluidine blue* | -0.08 | NS | 0.12 | NS |
| *Tidemark integrity* | 0.01 | NS | -0.03 | NS |
| sGAG | | | | |
| Medium | 13.86 | NS | 29.74 | $4.07x10^{-2}$ |

[a]FC is determined by the $2^{-\Delta\Delta CT}$ method and compared to its respective control. FC>1 is upregulation and FC<1 is downregulation. [b]Beta is determined by the GEE during the modelling and represents the difference between the perturbation and control group. [$] Significance of mean difference in gene expression between controls and treated explants were estimated by generalized estimating equation (GEE) with robust variance estimators to account for donor effects. Legend: FC=Fold change; IOP=iopanoic acid; NP=nanoparticle; MS=Mechanical stress; NS=Not significant; sGAG=sulphated glycosaminoglycans.

**Supplementary Table S4 | Gene expression measured by RT-qPCR and RNA sequencing between 65%MS+IOP in comparison to 65%MS.**

| | *RT-qPCR* | | *RNA-seq* | |
|---|---|---|---|---|
| **Gene** | **FC** | ***P*-value** | **FC** | ***P*-value** |
| ***MMP13*** | 0.10 | $1.73x10^{-4}$ | 0.06 | $9.00x10^{-3}$ |
| ***ADAMTS5*** | 0.43 | $2.16x10^{-2}$ | 0.84 | NS |
| ***EPAS1*** | 1.32 | NS | 1.01 | NS |
| ***COL2A1*** | 3.58 | $3.71x10^{-5}$ | 2.52 | NS |
| ***ACAN*** | 1.29 | NS | 1.06 | NS |
| ***COL1A1*** | 0.11 | *$5.29x10^{-2}$* | 0.02 | $4.72x10^{-4}$ |
| ***COL10A1*** | 0.23 | $1.05x10^{-3}$ | 0.18 | *$6.36x10^{-2}$* |
| ***ALPL*** | 0.03 | *$5.71x10^{-2}$* | 0.01 | $3.65x10^{-3}$ |

FC was calculated by the $2^{-ddCT}$ method in the RT-qPCR between 65%MS+IOP (n=11) and 65%MS (n=24). *P*-value in RT-qPCR was determined by performing a GEE. FC was calculated by DeSEQ for RNA-sequencing data between 65%MS+IOP (n=7) and 65%MS (n=14). *P*-value in the RNA-seq was determined by DESeq2 using a general linear model assuming a negative binominal distribution followed by a Wald-test. Legend: FC=Fold Change, RT-qPCR=real-time quantitative polymerase chain reaction; RNA-seq=RNA sequencing, NS=not significant.

**Supplementary Table S5 | Investigation of the 12 FDR significant genes in a consensome of thyroid signalling.**

| | 65%MS+IOP vs 65%MS | | | Thyroid signalling[b] | |
|---|---|---|---|---|---|
| **Gene** | **FC** | ***P*-value** | **FDR[a]** | **GMFC** | **CPV** |
| ***INSIG1*** | 3.25 | $6.12x10^{-6}$ | $2.24x10^{-2}$ | 1.20 | $1.59x10^{-4}$ |
| ***DHCR7*** | 2.92 | $1.47x10^{-5}$ | $3.28x10^{-2}$ | 1.27 | $1.42x10^{-11}$ |
| ***FADS1*** | 2.91 | $1.88x10^{-5}$ | $3.28x10^{-2}$ | 1.15 | $8.03x10^{-6}$ |
| ***LRP8*** | 2.87 | $3.75x10^{-5}$ | $4.58x10^{-2}$ | 1.13 | $5.15x10^{-3}$ |
| ***ACAT2*** | 2.25 | $1.55x10^{-5}$ | $3.28x10^{-2}$ | 1.17 | $1.91x10^{-5}$ |
| ***LTBP2*** | 0.43 | $2.01x10^{-5}$ | $3.28x10^{-2}$ | 1.12 | NS |
| ***CTGF*** | 0.35 | $3.78x10^{-6}$ | $2.24x10^{-2}$ | 1.38 | $1.46x10^{-7}$ |
| ***BMP5*** | 0.29 | $2.47x10^{-5}$ | $3.29x10^{-2}$ | 1.10 | NS |
| ***LOX*** | 0.23 | $4.14x10^{-6}$ | $2.24x10^{-2}$ | 1.26 | $1.17x10^{-2}$ |
| ***ADGRV1*** | 0.21 | $4.66x10^{-6}$ | $2.24x10^{-2}$ | 1.09 | NS |
| ***FOXM1*** | 0.16 | $1.74x10^{-5}$ | $3.28x10^{-2}$ | 1.15 | $3.28x10^{-5}$ |
| ***MASP1*** | 0.13 | $2.27x10^{-5}$ | $3.29x10^{-2}$ | 1.16 | $1.36x10^{-2}$ |

[a] To correct for multiple testing, the Benjamini-Hochberg method was applied to p-values and reported as the false discovery rate (FDR). [b] A consensome meta-analysis of thyroid manipulation studies summarizes genes involved in thyroid signalling [1]. Legend: FC=fold change; FDR= false discovery rate; GMFC= Geometric mean fold change; CPV=Consensome *P*-value.

# Supplementary Materials and Methods

### *1.1 Study design and patient participation*

Osteochondral explants were obtained from knee joints included in the Research in Articular Osteoarthritis Cartilage (RAAK) study [2]. The RAAK study has been approved by the medical ethical committee of the Leiden University Medical Center (P08.239/P19.013) and informed consent was obtained from subjects. Osteochondral explants were punched from the macroscopically preserved load bearing area of the femoral condyle of human OA knee joints and maintained in serum-free chondrogenic differentiation medium (DMEM, supplemented with Ascorbic acid (50 μg/ml; Sigma-Aldrich; Zwijndrecht, The Netherlands), L-Proline (40 μg/ml; Sigma-Aldrich), Sodium Pyruvate (100 μg/ml; Sigma-Aldrich), Dexamethasone (0.1 μM; Sigma-Aldrich), ITS+ and antibiotics (100 U/ml penicillin; 100 μg/ml streptomycin) in a 5% (v/v) CO2 incubator at 37°C [3]. Medium was refreshed every three to four days. In total 83 osteochondral explants were obtained from 16 donors for this study and divided over the treatment groups: control (n=30), injurious mechanical stress (65%MS; n=25), injurious mechanical stress treated with IOP (65%MS+IOP; n=11) and injurious mechanical stress treated with IOP encapsulated in PLGA NPs (65%MS+NP(IOP); n=17). Donor characteristics are summarized in **Supplementary Table 1**.



Patients and public were involved in the design, reporting and dissemination of the research via the patient, participation osteoArthritis Leiden (PPA-Leiden). PPA–Leiden consists of scientists of our research team and osteoarthritis patients that meet every 3 months. During meetings there is mutual exchange of information, reporting on progress, new research applications and discussions on research priorities. Reach out to broader public is via Facebook and Twitter. Dissemination of PPA-Leiden meetings is established by summary reports of meetings. As members of the PPA-Leiden are actively involved in other patient organizations such as poly-osteoarthritis society and the Dutch Arthritis Foundation this additionally allowed us to reach out to a broader OA patient population

### *1.2 RNA isolation, Reverse Transcription and quantitative Real-Time PCR*

Cartilage RNA was extracted by pulverizing the tissue using a Mixer mill 200 (Retch, Germany) and homogenizing in TRIzol reagent (Invitrogen, San Diego, CA). RNA was extracted with chloroform, precipitated with ethanol, and purified using the RNeasy Mini Kit (Qiagen, GmbH, Hilden, Germany). Genomic DNA was removed by DNase (Qiagen, GmbH, Hilden, Germany) digestion and quantity of the RNA was assessed using a Nanodrop spectrophotometer (Thermo Fischer Scientific Inc., Wilmington, USA). Synthesis of cDNA was performed using 200 ng of total mRNA with the First Strand cDNA Synthesis Kit (Roche Applied Science, Almere, The Netherlands) according to the manufacturer's protocol. Subsequently, pre-amplification was performed and gene expression was determined with the Roche Lightcycler 480 II (Roche Applied Science) using Fast Start Sybr Green Master mix (Roche Applied Science). To measure changes in chondrocyte signalling upon perturbations, we measured gene expression levels by RT-qPCR. Primer sequences used are listed in **Supplementary Table 2**. Fold changes (FC) were determined using the $2^{-\Delta\Delta CT}$ method, in which cyclic threshold (CT) levels were adjusted

for the housekeeping gene *SDHA* (-ΔCT) and subsequently for control samples (-ΔΔCT). A FC>1 represents an upregulation, while FC<1 depicts a downregulation. This endogenous reference genes were chosen based on literature stating the stability of this gene in response to mechanical stress [4,5].

### *1.3 RNA-sequencing*

#### *1.3.1 Quality control of sequencing data*

Paired-end 2x150 base pair RNA sequencing (Illumina TruSeq mRNA Library Prep Kit, Illumina HiSeq X ten) was performed. Strand specific RNA-sequencing libraries were generated which yielded on average 14 million reads per sample. Data from the Illumina platform was analysed with an in-house pipeline as previously described [6]. The adapters were clipped using Cutadapt v1.1. RNA-seq reads were then aligned using GSNAP against GRCh38 [7]. Read abundances per sample were estimated using HTSeq count v0.11.1 [8] with Ensembl gene annotation version 94. Only uniquely mapping reads were used for estimating expression. The quality of the raw reads and initial processing for RNA-sequencing was checked using MulitQC v1.7 [9]. Samples containing >50% genes with zero values and average read count <10 were removed from further analysis. To identify outliers, principal component analysis (PCA) was applied and identified two clusters which were independent of treatment and hence analysis was performed with corrections for principal component 1.

#### *1.3.2. Differential expression analysis and protein-protein interactions*

Differential expression analysis was performed in 65%MS+IOP cartilage compared to 65%MS cartilage obtained from osteochondral explants using DESeq2 R package version 1.24 [10] on 14.668 protein-coding genes. A general linear model assuming a negative binominal distribution was applied and followed by a Wald-test between 65%MS+IOP and 65%MS samples with correction for principal component 1. In all analyses, 65%MS samples were set as reference. To correct for multiple testing the Benjamini-Hochberg method was used, as indicated by the false discovery rate (FDR) in which a significant cut-off value of 0.05 was used. For protein-protein interactions, analysis was performed using the online tool STRING version 11.0 [11].

#### *1.3.3 RNA-sequencing validation by Real-time quantitative PCR (RT-qPCR)*

For validation and replication a total of 8 paired samples were selected. 200 ng of RNA was processed into cDNA using the First Strand cDNA Synthesis Kit (Roche Applied Science, Almere, The Netherlands). Real-Time qPCR was performed and normalized as described above to determine gene expression of *INSIG1*, *DHCR7*, *FADS1, CTGF*, *BMP*5 and *FOXM1*. Primer sequences are listed in **Supplementary Table 2.**

### *1.4 Determining cartilage integrity*

#### *1.4.1 Sulphated glycosaminoglycan (sGAGs) measurement*

Sulphated glycosaminoglycans (sGAGs) concentration was measured in conditioned media of explants on day 13 following extraction with the photometric 1,9 dimethylene blue (DMMB; Sigma-Aldrich) dye method [12]. Shark chondroitin sulfate (Sigma-Aldrich) was used as the reference standard. To measure concentrations, 100µl of medium or digested cartilage was mixed with 200µl of DMMB solution and the absorbance at 525nm and 595nm was measured in a microplate reader (Synergy HT; BioTek, Winooski, USA).

#### *1.4.2 Histology*

Osteochondral explants were fixed in 4% formaldehyde for one week and decalcified using EDTA (12,5%, pH=7.4) for two weeks at 4°C. Subsequently, samples were dehydrated with an automated tissue processing apparatus and embedded in paraffin. Tissue sections of 5 µm were stained with Hematoxylin and Eosin (H&E) or toluidine blue (Sigma-Aldrich) and mounted with Pertex (Sigma-Aldrich). Quantification of OA related cartilage damage was scored according to Mankin *et al* [13].



### *1.5 Preparation and characterization of nanoparticles (NPs)*

#### *1.5.1 Preparation of PLGA-PEG NPs*

PLGA NPs with entrapped iopanoic acid (IOP) and near-infrared fluorescent labels was prepared using an o/w emulsion and solvent evaporation-extraction method [14]. In brief, 100 mg of PLGA in 3 mL of DCM containing IOP (2mg; Sigma Aldrich) and Indocyanine green (1mg; ICG) was added dropwise to 25 mL of aqueous 2% (w/v) PVA in distilled water and emulsified for 90 seconds using a sonicator (Branson, sonofier 250). A lipid mPEG 2000 PE (20 mg) was dissolved in DCM and added to the vial. The DCM was removed by a stream of nitrogen gas. Subsequently, the emulsion was rapidly added to the vial containing the lipids and the solution was homogenized during 30 seconds using a sonicator. Following overnight evaporation of the solvent at 4°C, the PLGA NPs were collected by centrifugation at 10,000 g for 10 min, washed three times with distilled water and lyophilized.

#### *1.5.2 Encapsulation Efficiency Analysis*

In order to determine the encapsulating efficiency (EE) and the loading content of the IOP and near infrared dye (ICG), the lyophilized NPs were dissolved in 0.8 M NaOH. Separately, 5 mg of PLGA NPs were dissolved in in 0.5 mL 0.8 M NaOH overnight at 37°C. Afterwards, the basic solutions of all the NPs were centrifuge at 13.8 g, at RT for 20 min and the supernatants were collected. The IOP content was determined by RP-HPLC and the ICG dye content was then measured using Odyssey Infrared Imager 9120 (LI-COR) scanner with a 800nm scan. NIR dye encapsulation efficiency was calculated following a previously described [15] formula as following:

$$EE = \frac{Amount\ of\ drug\ in\ formulation}{Amount\ of\ drug\ used\ for\ formulation} x100$$

*Amount of drug in formulation* is the amount of IOP and ICG loaded in the PLGA NPs. The values were obtained as previously described. *Amount of drug used for formulation* is the amount of IOP and NIR added in the preparation of NPs.

### *1.5.3 Particles size and charge surface*

The average size and polydispersity index (PDI) of the PLGA NPs were determined by Dynamic Light Scattering (DLS) (Zetasizer Nano S90, Malvern Instruments, Worcestershire, UK). PLGA NPs were dissolved in MilliQ water and the measurement was performed at 25 °C at an angle of 90°. The values presented are averages and standard deviations of triplicate measurements. The stability and the aggregation in a dispersion NPs was determined by Zeta potential (Zetasizer Nano S90, Malvern Instruments, Worcestershire, UK) (**Table 1**).

**Table 1 | Characterization of PLGA nanoparticles used in this study.**

| Nanoparticles | Particles size (nm±stdev) | Polydispersity | Zeta potential (mV) | EE% (ICG) | EE% (IOP) |
|---|---|---|---|---|---|
| 1-PLGA-NP-(ICG)-PEG | 256 ± 0.85 | 0.176 ± 0.08 | -12.2 | 8.8 | 29.6 |
| 2-PLGA-NP-(IOP)-PEG | 265 ± 0.67 | 0.185 ± 0.06 | -14.6 | 9.4 | 31.0 |

PLGA NPs size, polydispersity, zeta potential, fluorescent dye and drug encapsulation efficiency (EE) of PLGA NPs

### *1.5.4. Release of IOP from NPs*

Release of IOP from NPs was measured by maintaining 150µl of 5mg/ml NP at 21°C or 37°C under slight shaking. On each time point, NPs were centrifuged (12.000 rpm) for 10 minutes and PBS was carefully taken for subsequent IOP concentrations measurement using a Nanodrop spectrophotometer (Thermo Fischer Scientific Inc., Wilmington, USA) at 310nm (**Supplementary Figure S1C**).

## *1.6 In vitro experiments.*

### *1.6.1 Cell culture.*

Human primary chondrocytes were cultured in DMEM (High glucose) supplemented with 10% fetal calf serum (FBS; Gibco, Bleiswijk, The Netherlands), 0.5 ng/ml FGF-2 (PreproTech, Heerhugoweaard, The Netherlands) and antibiotics (100U/ml penicillin; 100µg/ml streptomycin; Gibco) in a 5% (v/v) $CO_2$ incubator at 37°C.

### *1.6.2 NP uptake study.*

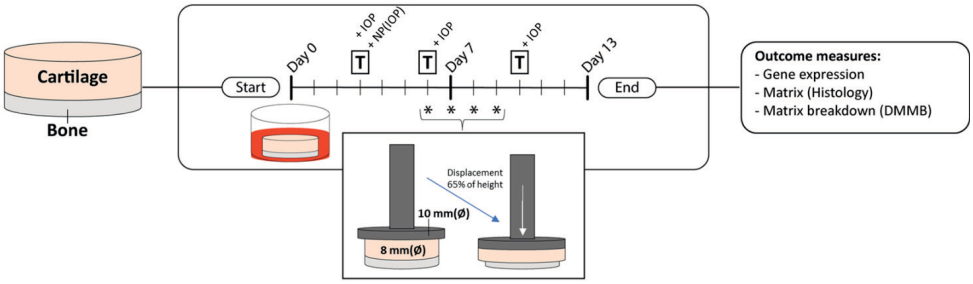
Subsequently, cells were seeded in a 96-well cell culture microplate (Greiner Bio-One B.V. Alphen aan den Rijn, The Netherlands) (1x10$^6$ cells/well) and incubated with 1.6 µl of 5mg/ml Indocyanine green (ICG) loaded PLGA-PEG NPs for 1h, 4h and 24h. In short, after incubation, cells were washed twice with PBS, fixed for 15 minutes with 1% paraformaldehyde, washed

with PBS and subsequently, stained with TO-PRO©-3 iodide dye (ThermoFisher, Marietta, OH, USA) to stain cell nucleus at 700 nm. Uptake of NPs by cells was measured using an Odyssey Infrared Imager 9120 (LI-COR, Lincoln, NE, USA) scanner at 800 nm and 700 nm intensity to visualize the NPs and cells, respectively (**Supplementary Figure S2A**). This experiment was performed in triplicate (n=3).

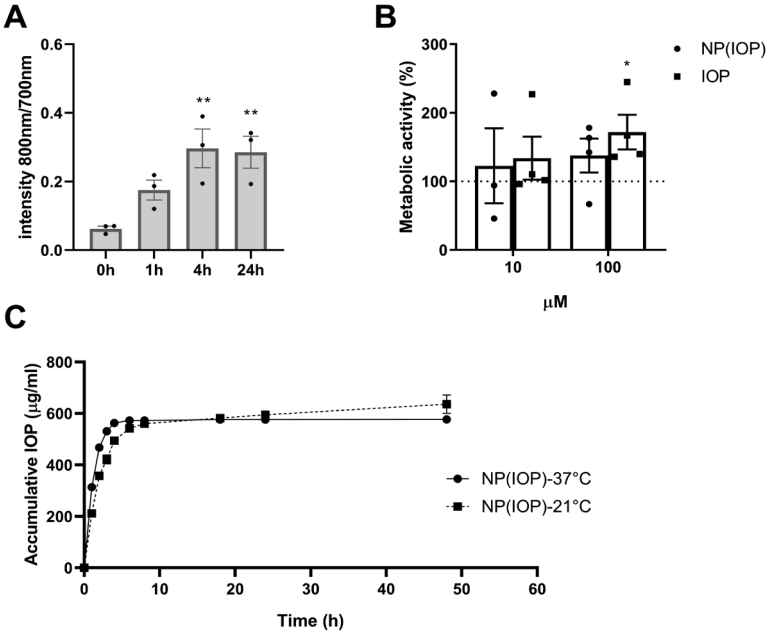
### *1.6.3 Cell viability assay.*

Effects of 8 and 80 μg/ml NP(IOP) and 10μM and 100μM IOP on cell metabolism was investigated using a chondrosarcoma cell line CH2879 (**Supplementary Figure S2B**) [16,17]. CH2879 cells were cultured in RPMI 1640 (HEPES, L-glutamine, Gibco) supplemented with 10% fetal calf serum (FBS; Gibco and antibiotics (100U/ml penicillin; 100μg/ml streptomycin; Gibco). Cells were seeded (16.000 cells/well) in a 96 well cell culture microplate (Greiner Bio-One B.V. Alphen aan den Rijn, The Netherlands). 24hrs after seeding cells, respective treatments were added. Subsequently, 24hrs after treatment, Alamar Blue (Invitrogen) was added to the wells at a final concentration of 10% and incubated for 4hr in a 5% (v/v) $CO_2$ incubator at 37°C. Fluorescence was measured using an excitation of 544nm and emission of 590nm with a spectrometer (PerkinElmer). This experiment was performed in quadruplicate (n=4).

# Supplementary Figures




**Supplementary Figure S1 | Schematic representation of study setup.** Osteochondral explants were punched from the still macroscopically preserved looking knee condyle area and taken into culture. Explants were treated with IOP (100µM) or PLGA NP-IOP from day 3 onwards. Asterix depicts days explants received mechanical stresses at a strain of 65% for 10 min per day. Media was collected on the with T indicated days and subsequently each explant received fresh media. Finally, on day 13, a sagittal section was fixed in 4% formaldehyde for histology, while for the remaining explant cartilage and bone was separated, snap frozen and stored at -80C for downstream analyses. Legend: NP=Nanoparticles, IOP=iopanoic acid, DMMB=Dimethylmethylene Blue Assay.




**Supplementary Figure S2 | Characterization of PLGA-PEG nanoparticles. [A]** *In vitro* cellular uptake of PLGA-PEG nanoparticles of primary chondrocytes characterized by Odyssey. Bars represent the mean ± s.e.m and n=3. **[B]** Metabolic activity upon 24h treatment with 10µM or 100µM of IOP in nanoparticles and free IOP was measured using Alamar Blue assays in CH2874 cell lines. Viability of untreated controls is depicted by the dashed line and was set to represent 100% cell viability. Bars represent the mean ± s.e.m. **[C]** Release of IOP from nanoparticles over time measured at 21°C and 37°C. Asterisks represent significant differences as measured by one way ANOVA. *p<0.05; **p<0.01. n=3 or n=4. Legend: IOP=iopanoic acid; NP=nanoparticles

# REFERENCES


1. Ochsner SA, McKenna NJ. No Dataset Left Behind: Mechanistic Insights into Thyroid Receptor Signaling Through Transcriptomic Consensome Meta-Analysis. *Thyroid*. 2020;30(4):621-39.
2. Ramos YF, den Hollander W, Bovee JV, et al. Genes involved in the osteoarthritis process identified through genome wide expression analysis in articular cartilage; the RAAK study. *PLoS One*. 2014;9(7):e103056.
3. Houtman E, van Hoolwerff M, Lakenberg N, et al. Human Osteochondral Explants: Reliable Biomimetic Models to Investigate Disease Mechanisms and Develop Personalized Treatments for Osteoarthritis. *Rheumatol Ther*. 2021;8(1):499-515.
4. Al-Sabah A, Stadnik P, Gilbert SJ, et al. Importance of reference gene selection for articular cartilage mechanobiology studies. *Osteoarthritis Cartilage*. 2016;24(4):719-30.
5. McCulloch RS, Ashwell MS, O'Nan AT, et al. Identification of stable normalization genes for quantitative real-time PCR in porcine articular cartilage. *J Anim Sci Biotechnol*. 2012;3(1):36.
6. Coutinho de Almeida R, Ramos YFM, Mahfouz A, et al. RNA sequencing data integration reveals an miRNA interactome of osteoarthritis cartilage. *Ann Rheum Dis*. 2019;78(2):270-7.
7. Wu TD, Watanabe CK. GMAP: a genomic mapping and alignment program for mRNA and EST sequences. *Bioinformatics*. 2005;21(9):1859-75.
8. Anders S, Pyl PT, Huber W. HTSeq--a Python framework to work with high-throughput sequencing data. *Bioinformatics*. 2015;31(2):166-9.
9. Ewels P, Magnusson M, Lundin S, et al. MultiQC: summarize analysis results for multiple tools and samples in a single report. *Bioinformatics*. 2016;32(19):3047-8.
10. Love MI, Huber W, Anders S. Moderated estimation of fold change and dispersion for RNA-seq data with DESeq2. *Genome Biol*. 2014;15(12):550.
11. Szklarczyk D, Gable AL, Lyon D, et al. STRING v11: protein-protein association networks with increased coverage, supporting functional discovery in genome-wide experimental datasets. *Nucleic Acids Res*. 2019;47(D1):D607-D13.
12. Farndale RW, Buttle DJ, Barrett AJ. Improved quantitation and discrimination of sulphated glycosaminoglycans by use of dimethylmethylene blue. *Biochim Biophys Acta*. 1986;883(2):173-7.
13. Mankin HJ, Dorfman H, Lippiello L, et al. Biochemical and metabolic abnormalities in articular cartilage from osteo-arthritic human hips. II. Correlation of morphology with biochemical and metabolic data. *J Bone Joint Surg Am*. 1971;53(3):523-37.
14. Cruz LJ, Tacken PJ, Fokkink R, et al. Targeted PLGA nano- but not microparticles specifically deliver antigen to human dendritic cells via DC-SIGN in vitro. *J Control Release*. 2010;144(2):118-26.
15. Rosalia RA, Cruz LJ, van Duikeren S, et al. CD40-targeted dendritic cell delivery of PLGA-nanoparticle vaccines induce potent anti-tumor responses. *Biomaterials*. 2015;40:88-97.
16. Gil-Benso R, Lopez-Gines C, Lopez-Guerrero JA, et al. Establishment and characterization of a continuous human chondrosarcoma cell line, ch-2879: comparative histologic and genetic studies with its tumor of origin. *Lab Invest*. 2003;83(6):877-87.
17. van Oosterwijk JG, Herpers B, Meijer D, et al. Restoration of chemosensitivity for doxorubicin and cisplatin in chondrosarcoma in vitro: BCL-2 family members cause chemoresistance. *Ann Oncol*. 2012;23(6):1617-26.


PEBP1
MBIP
KAT2B
RCC2
TET1
TYRO3
CDKN1C
KLF2
GADD45
SOCS3
CD9
CDA
SES1
MYC
ENG
GAPDH
PRKAG2
NFKBIA
CAV1
CYR61
EHD3
FKBP5
CMBL
TSC22D3
MXRA5
PSAT1
GSN
WARS
LRRC16A
SCUBE1
ALDH1L1
TNC
ITM2A
ITGA10
RPL10A
RPS12
RIOK3
NEK6
CNTFR
CRLF1
RCAN2
SOCS2
LPIN1
HTRA1
IGFBP4
IGFBP3
STC2
IGFBP7
IGFBP5
SERPINE1
ADAM12
MMP13
FRZB
PTGS
AMFR
EDEM1
OS9
IARS
SLC25A5
TLN2
RGCC
DP2